

# EXPERIMENTAL STUDY ON FLASHING-INDUCED INSTABILITIES IN AN OPEN NATURAL CIRCULATION SYSTEM

Yuliang Fang<sup>1,2,3</sup>, Xiixin Cao<sup>2</sup>, Wenxi Tian<sup>1</sup>

1. School of Nuclear Science and Technology, Xi'an Jiaotong University, Xi'an, China
2. College of Nuclear Science and Technology, Harbin Engineering University, Harbin, China
3. Tianjin Institute of Power Sources, CETC, Tianjin, China

## ABSTRACT

The natural circulation system (NCS) uses gravity pressure drop caused by density differences in the loop to generate the driving force without any external mechanical devices, which has been widely applied to the design of the nuclear reactor system and the passive safety system due to its simple structure, high intrinsic safety, and strong heat discharge capacity. However, the low-pressure condition can lead to a two-phase flow and make the flow characteristics in the NCS more complex. Flashing-induced instability occurring in the open NCS will cause the system structural vibration as well as mechanical damage and bring safety problems. The study on flashing-flow behaviors in an open NCS has been conducted experimentally in this paper. High-speed camera, thermal needle probe and wire-mesh sensor were adopted to record the flow pattern and measure the void fraction in the polycarbonate visualization riser section. In the start-up process, with the inlet temperature in the riser section increasing, the open NCS has experienced single-phase stable flow, intermittent oscillation between single-phase and two-phase, high subcooling two-phase stable flow, flashing-induced instabilities flow, and low subcooling two-phase stable flow. The flow pattern evolution of flow flashing goes through bubble flow, cap-slug flow, churn flow and wispy annular flow, in which the length of churn can account for more than 40% length of the two-phase regime. The flash number  $N_{flash}$  is used to divide the region of flashing-induced instabilities. It is found that the open NCS is in a stable two-phase flow when the flash number at the outlet of the riser section  $N_{flash,out} = 4\sim 5$ .

Keywords: Natural circulation; flashing-induced instabilities; experiment; flow pattern evolution

## NOMENCLATURE

$c_p$	specific heat capacity, J/kg/K
$h$	specific enthalpy, J/kg
$m$	circulation flow, kg/s
$P$	pressure, kPa
$\Delta P$	pressure drop, kPa
$\dot{Q}$	heat power, kW
$T$	temperature, K
$\alpha$	void fraction
$v$	specific volume, m <sup>3</sup> /kg
$\tau$	period, s
$\Delta$	uncertainty
Subscript	

$f$	liquid
$g$	vapor
$fg$	D-value between the liquid and the vapor
$in$	inlet
$s$	saturation
Abbreviation	
FII	Flashing-Induced Instabilities
NCS	Natural Circulation System
LUNAR	Low-pressure NATURAL ciRculation

## 1. INTRODUCTION

Natural circulation is a passive heat transport form which uses density differences to generate the driving force. The open natural circulation system (NCS) is with low pressure, simple structure, high intrinsic safety, and strong heat discharge capacity, which has been widely applied to new advanced nuclear reactor systems and passive safety systems<sup>1</sup>. However, the two-phase flow due to the low pressure makes the flow characteristics more complex in the NCS. Flashing occurs in the riser section and even induces flow instability which can lead to NCS safety problems, such as structural vibration and damage.

Many investigations have been conducted about flashing-induced instabilities (FII) in the NCS over the past few decades by theoretical analysis, experiments and CFD calculation. Although the previous flashing flow models are not quite perfect, new advances<sup>2</sup> have been made in modelling phase change mechanisms, bubble dynamics and interfacial slip and interphase transfer. The mechanisms and models of flashing two-phase flow were summarized on nucleation, flashing inception and bubble growth<sup>2-4</sup>. Van Bragt et al.<sup>5</sup> and Hu et al.<sup>6</sup> developed a dynamic model for FII in natural circulation BWRs under low-pressure conditions. Hou et al.<sup>7</sup> derived a theoretical formula to determine the flashing flow behavior of a flashing-driven NCS by using a quasi-linear flashing mode in which the prediction results were validated by experimental data. It is very important for improving closure models to acquire high-resolution and high-quality experimental data, which are lacking in most experiments.

Since the FII was first observed by Wissler, many natural circulation facilities have been established to study this phenomenon, like CIRCUS<sup>8</sup>, GENEVA<sup>9</sup>, PUMA<sup>10</sup>, SIRIUS-N<sup>11</sup>, HEU-PCCS<sup>12</sup> and so on. The different FII types were observed and recorded in the experiments. The mechanism and stability maps were presented by researchers. Qi et al.<sup>13</sup> indicated there

are five flow types in the open NCS: single-phase stable flow, flash and geyser coexisting unstable flow, flash stable flow, flash unstable flow, and flash and boiling coexisting unstable flow. Some factors on the flow characteristics of the NCS were performed, like heat power, inlet subcooled and cooling tank level. In addition, various numerical methods and analysis codes were developed for analyzing the flashing-induced instabilities in the NCS, such as FLOCAL<sup>14</sup> and RELAP5<sup>15,16</sup>.

In this study, the flashing-driven open natural circulation loop was established to explore the flashing-induced instabilities. This paper contributes to the fundamental understanding of flashing-induced instabilities and the design of low-pressure natural circulation systems, such as the passive containment cooling system, the natural-circulation-driven novel modular reactor system, and so on.

## 2. EXPERIMENTAL TEST LOOP AND METHODS

### 2.1 Experimental Test Loop

The Low-pressure NATural ciRculation (LUNAR) loop is an open loop<sup>1</sup>, as shown in Figure 1, including an open water tank, polycarbonate visual riser section, downcomer, preheater, forced-circulation bypass loop, water supply system and so on. The main performance parameters of the LUNAR loop are listed in Table 1.

In LUNAR loop, nine Type T thermocouples (T1~T9) are arranged in the riser section to measure the fluid temperatures. Thermal needle probes and the wire-mesh sensor is located between thermocouples to measure the distribution of void fraction. Pressure transducers (P1 and P2) are installed in the lower part of the riser and downcomer section respectively, and P3 is in the same height position as T8. The pressure taps of differential pressure transducer  $\Delta P2$  are on the position of P1 and P2, while  $\Delta P1$  located between P1 and T9 measures the pressure drop of the rising section. The open water tank is used as the heat sink, located at the upper part of the LUNAR loop, and the electric preheater in the horizontal section provides thermal power as the heat source. The circulation flow rate has been measured by an electromagnetic flowmeter.

**TABLE 1: PERFORMANCE PARAMETERS OF THE LUNAR LOOP**

Parameter	Value
System pressure [MPa]	0.1
Fluid temperature [°C]	15~110
Water tank level [cm]	15~70
Total height of the LUNAR loop [m]	6.50
Height of the riser section [mm]	5430
Inner diameter of riser section [mm]	50
Heating power [kW]	0~60
Heating rod size [mm]	$\Phi 12 \times 800$
Number of heating rods	60
Inner diameter of heater [mm]	DN350

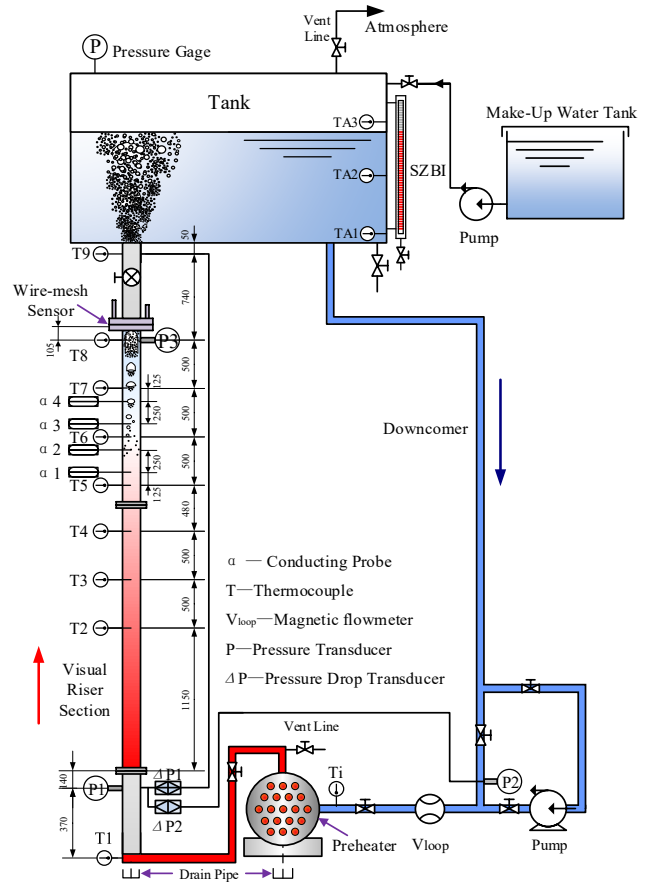


**FIGURE 1: SCHEMATIC OF THE LUNAR LOOP**

When the LUNAR loop starts, the water is heated by the horizontal preheater. The fluid density decreases after passing through the electric heater, which forms the driving force between the upward and downward sections to promote fluid flow. The pump of the bypass loop provides the initial driving force to overcome the flow resistance. The parameters of the measuring instruments are shown in Table 2.

**TABLE 2: PARAMETERS OF THE MEASURING INSTRUMENTS**

Instrument	Range	Accuracy
Type T thermocouple [°C]	-40~125	0.5
Pressure transducers [kPa (abs)]	0~250	0.20
Differential pressure transducer [kPa]	0~20	0.055%
Flowmeter [m <sup>3</sup> /h]	0~23	0.045%
TNP/WMS [ $\mu\text{S}/\text{cm}$ ]	0.05~500	—
Level gauge [mm]	0~700	$\pm 10$
NI acquisition system	—	0.2%

### 2.2 Experimental Uncertainty

Uncertainty analysis has been undertaken to evaluate the reliability and accuracy of experimental data. According to the sources of error, uncertainty  $\Delta$  can be classified into type A  $\Delta_A$

and type B  $\Delta_B$ . Type A uncertainty is assessed by statistical analysis of measured data, which is usually expressed by sample standard deviation  $S$ . Type B uncertainty is the uncertainty whose error comes from measuring instruments and acquisition devices.

$$\Delta = \sqrt{\Delta_A^2 + \Delta_B^2} = \sqrt{S^2 + \Delta_{sys}^2} \quad (1)$$

$$\Delta_{sys} = \sqrt{\Delta_{mea}^2 + \Delta_{acq}^2} \quad (2)$$

where  $\Delta_{mea}$  and  $\Delta_{acq}$  can be calculated by the accuracy of measuring instruments and acquisition devices. The uncertainty of experimental data is shown in Table 3.

**TABLE 3: UNCERTAINTY OF EXPERIMENTAL DATA**

Parameter	$\Delta/\%$
Fluid temperature	0.64~7.23
Pressure	5.26~15.83
Pressure drop	0.24~13.64
Flow rate	0.62~6.68
Void fraction	3.87~9.41

### 3. RESULTS AND DISCUSSION

During the LUNAR loop running, the subcooling degree of single-phase fluid in the riser section decreases gradually after being heated. It is shown that four flow modes appear in the low-pressure natural circulation system, including the single-phase steady flow, intermittent oscillation between single-phase and two-phase, flashing-induced oscillating flow and flashing-induced steady two-phase flow.

#### 3.1 Intermittent Oscillation Between Single-Phase And Two-Phase

Figure 2 and Figure 3 present the transition process from single-phase flow to two-phase flow under the heated power of 40 kW and the water tank level of 45 cm. With the fluid being heated continuously, the water temperature at the outlet of the preheater rises but does not reach saturation. When the subcooled fluid flows up from the riser inlet, the pressure head drops and the fluid temperature reaches or exceeds the saturation temperature under local pressure, and then the flow flashing occurs. Gradually, the flashing develops from the top to the bottom of the riser section due to the pressure dropping in the two-phase region, as shown in Figure 2. The flashing makes the liquid phase change into the vapor phase so that the vapor fraction in the riser section increases while the fluid density decreases, greatly increasing the driving force and the circulating flow of the loop. At the same time, the increase in circulation flow leads to more subcooling water flowing into the preheater. The preheater cannot heat the subcooling fluid to the temperature of flashing occurring just now in time, so the fluid temperature at the outlet of the preheater decrease. The flashing gradually disappears upward, which causes the reduction of the flashing driving force and loop flow. One oscillation between single-phase and two-phase period ends when the inlet temperature of

the riser section reaches the minimum. In this flow instability type, two-phase flow alternates with single-phase flow.

However, the water in the water tank is not saturated, and the flashing inception could move up and down a few times. The unstable oscillation process is dynamic and intermittent with a nearly stable period. In the LUNAR loop, the intermittent oscillation between single-phase and two-phase occurs 4~6 times whose average period is about 150 s. Every period is a process of energy storage and release, where the longer the energy storage period is, the higher the circulation flow is. In addition, the oscillation amplitude increases first and then decreases, in which the third or fourth oscillation amplitude is the highest. Intermittent oscillation comes to an end and the circulation flow nearly approaches a steady state when the fluid temperature in the water tank gradually reaches saturation. At this time, the inlet temperature of the preheater is basically unchanged where the fluid subcooling degree is approximately 11~12 °C.

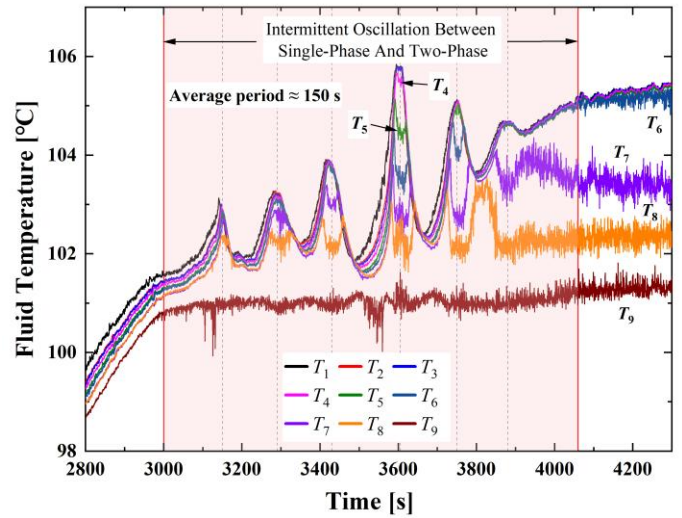


**FIGURE 2: FLUID TEMPERATURE DISTRIBUTION IN THE RISER SECTION**

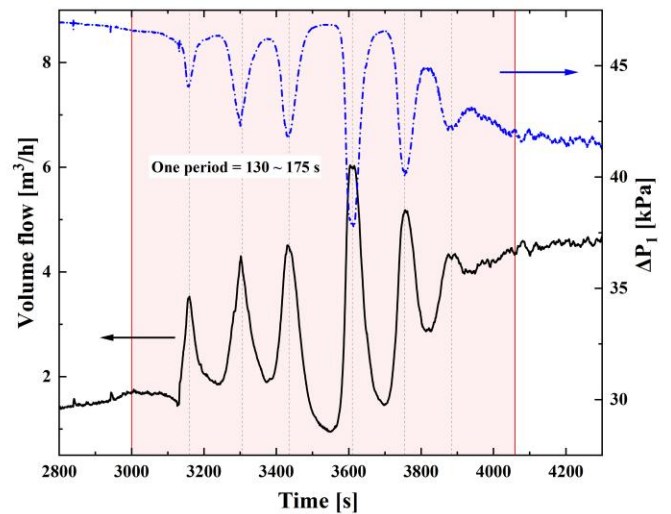


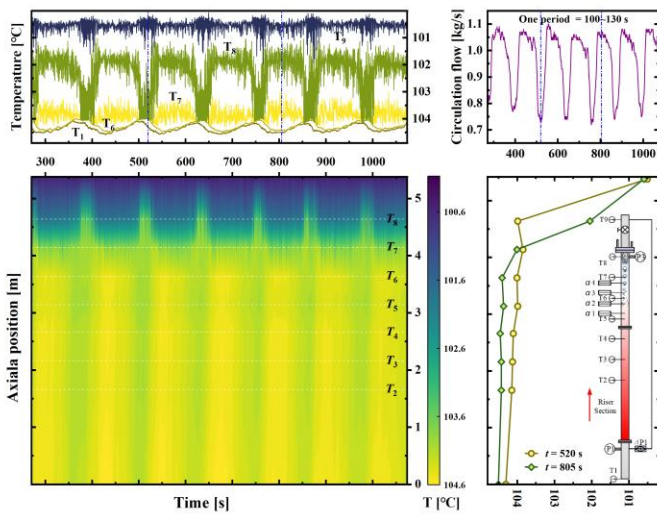
**FIGURE 3: LOOP CIRCULATION FLOW AND PRESSURE DROP OF THE RISER SECTION**

It is also found that the position of flashing inception can be affected by the nucleation site density and fluid superheat. The fluid is in an overheated state of about 0~1.5 °C at the position of flashing inception. What's more, the inserts in the riser section, like thermocouples and probes, can provide a large number of nucleation sites to make flashing inception develop downwards obviously.

### 3.2 Flashing-induced Oscillation Flow

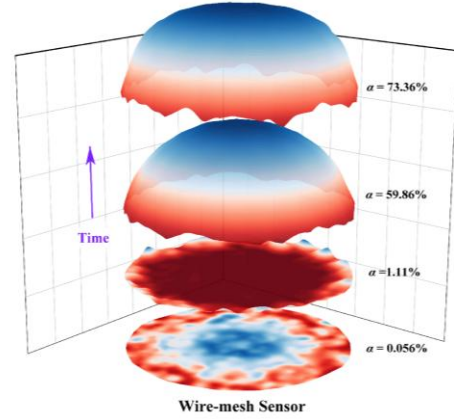
Flashing-induced oscillation flow occurs when the low subcooled degree fluid flows into the riser section. Compared with the intermittent oscillation between single-phase and two-phase, the process of the flashing-induced oscillation is similar but the water in the tank is almost saturated and two-phase flow is always present in the system.

This flow instability is periodic, intermittent, and with a nearly constant amplitude, as Figure 4 shows. Under the inlet temperature of 104.4 °C in the riser section and the water tank level of 27 cm, the time of every peak is longer than that of the trough and one oscillation period is about 100~130 s, which is mainly affected by the water tank level and inlet subcooling. The fluid temperatures in the riser section are fluctuating during every period where the single-phase fluid temperatures of the riser section fluctuate by about 0.5 °C and the two-phase fluid temperatures are affected by both the flashing-induced instability and the local flashing process. In addition, the inlet and outlet temperatures in the riser section are out-of-phase. The flashing inception changes periodically between the position of T6 and T8. Two-phase flow always exists in the riser section as T9 exhibits the saturation temperature of the local pressure. The main reason for this intermittent flashing instability is that the input and output heat of the natural circulation system does not match, and the driving force and flow resistance are dynamically adjusted.



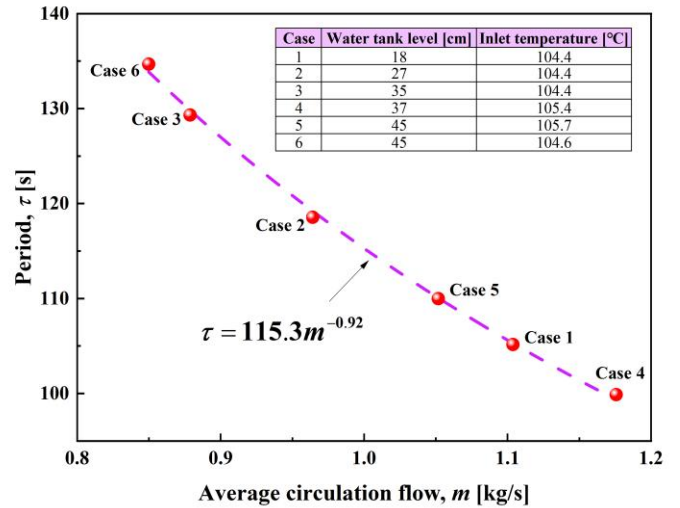
**FIGURE 4: FLUID TEMPERATURE AND LOOP CIRCULATION FLOW OF THE RISER SECTION**

Figure 5 shows the void fraction evolution process during one oscillation period. It is found that the small bubbles occur when the flashing begins and develop bigger near the wall. Little by little the big bubble or steam slug is close to the cross-section center and evolves into churn flow or others. The radial distribution of the void fraction is smoother when the flashing reaches the peak.



**FIGURE 5: VOID FRACTION DISTRIBUTION RECONSTRUCTED BY WIRE-MESH SENSOR**

In Figure 6, the oscillation period of six experimental cases is displayed against the average circulation mass flow. It should be pointed out that the period of the flashing-induced oscillation flow varies in direct proportion with a -0.92 power of the average circulation mass flow. As Manera<sup>14</sup> indicated, this relation is only influenced by the system structure rather than heat power, operating pressure or inlet subcooling.



**FIGURE 6: OSCILLATION PERIOD VS. AVERAGE CIRCULATION FLOW**

The dimensionless numbers, like the subcooling number  $N_{sub}$  and the phase change number  $N_{pch}$ , are usually adopted to delimit the flow instability boundary. The  $N_{sub}$  and  $N_{pch}$  are defined as follows:

$$N_{sub} = \frac{h_{s,in} - h_{f,in}}{h_{fg,in}} \frac{v_{fg,in}}{v_{f,in}} \quad (3)$$

$$N_{pch} = \frac{Q}{mh_{fg,in}} \frac{v_{fg,in}}{v_{f,in}} \quad (4)$$

where  $Q$  is the effect heat power and calculated by the product of circulation flow and enthalpy difference between the inlet and outlet of the preheater. The relation between the inlet subcooling number  $N_{sub}$  and phase change number  $N_{pch}$  of the riser section is shown in Figure 7. Although the sample time is different, the results of six cases imply that the  $N_{sub,in}$  is a linear function of the  $N_{pch,in}$ . The flashing-induced oscillation boundary is also presented in Figure 7.

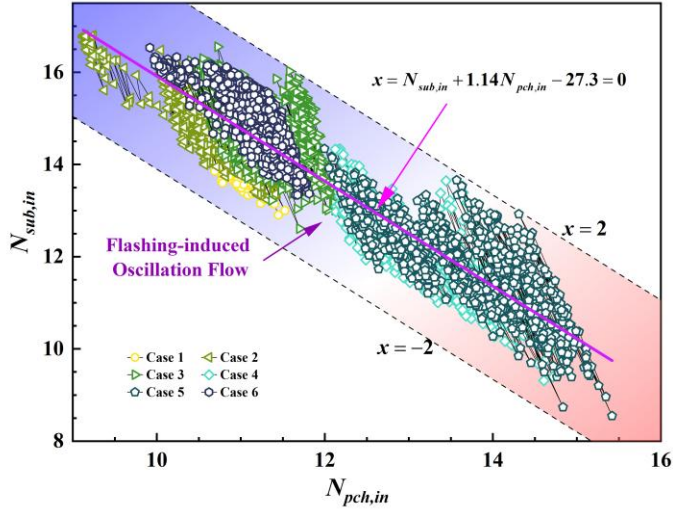


**FIGURE 7: INLET SUBCOOLING NUMBER VS. PHASE CHANGE NUMBER OF THE RISER SECTION**

Ishii introduced the flashing number  $N_{flash}$  to explore the mechanism of the flashing flow. This number weighs up the degree of the flashing flow development by the vapor fraction.

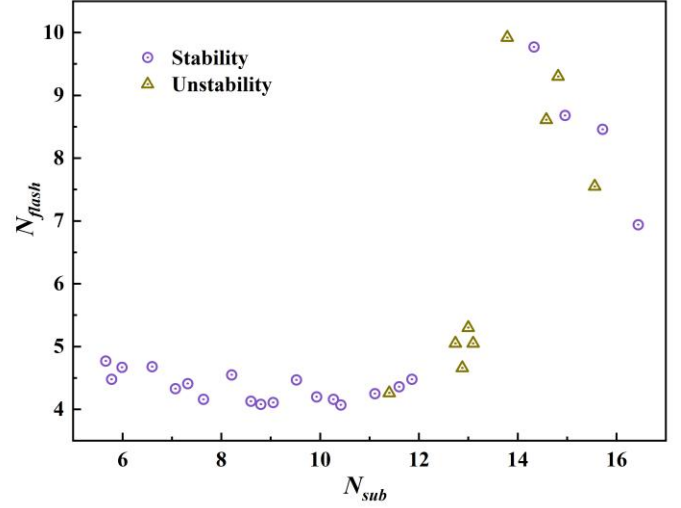
$$N_{flash} = \frac{c_{p,f}(T_{in}-T_s)}{h_{fg}} \frac{v_{fg}}{v_f} (1 - \alpha) \quad (5)$$

This flashing number is adopted to evaluate the flashing-induced instability in this work. Figure 8 presents the new flow instability map of the open natural circulation system in which the outlet vapor fraction of the riser section is used to calculate the  $N_{flash}$ . It is shown clearly that the  $N_{flash}$  for the flashing-induced steady two-phase flow is within 4~5 when the  $N_{sub} < 12$ . When the  $N_{sub}$  is relatively high, the two-phase flow section is very short and the outlet vapor fraction is very small. The flow pattern of the two-phase section is the bubble flow and the driving force for natural circulation flow is mainly generated by the density difference of the single-phase section between the riser section and the downcomer section. Accordingly, the natural circulation system is in a stable flow state.

### 3.3 Flashing Flow Pattern Evolution

Flow flashing is a phase change process like flow boiling, but they differ marginally. The flashing inception depends on the nucleation site location and can occur inside the liquid or on the wall. Therefore, once there are enough nucleation sites when the fluid is saturated or overheated, metastable liquids will vaporize at the nucleation site location due to the thermodynamic non-equilibrium effect. That is, the thermodynamic non-equilibrium

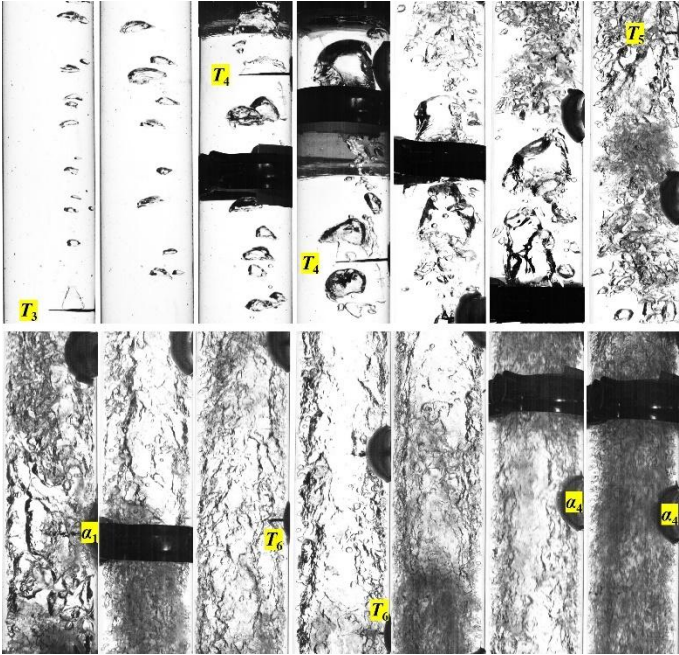
effect is a sufficient condition to induce flashing vaporization, and the existence of nucleation sites is a necessary factor to promote flashing vaporization. At the same time, the flow pattern evolution of flow flashing is also closely related to flow stability.



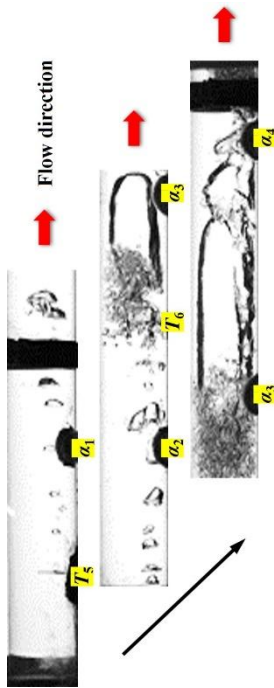
**FIGURE 8: FLOW INSTABILITY MAP**

Figure 9 exhibits the flow pattern evolution of steady flashing flow recorded by the high-speed camera under the inlet temperature of 107 °C in the riser section, the water tank level of 18 cm, and the circulation flow rate of 0.83 m/s. In this experiment, the bubble production process on the wall is not observed clearly due to the smooth wall and the effect of transmittance but occurs on the surface of the inserted thermocouple. On the one hand, the metal surface of the thermocouple provides the nucleation sites, and on the other hand, disturbed flow caused by the superheated fluid flowing around the thermocouple accelerates this flashing process. The flame-shaped bubble on the thermocouple surface is constantly torn and separated in the tail, forming a small bubble flow.

The separation bubbles develop from an ellipsoid shape to an irregular shape with a smooth tail and convex top, with a diameter of 5~20 mm. Bubbles grow up gradually in the upward flow, and adjacent bubbles collide, break up and coalesce. As the fluid flows upwards and the static pressure gradually decreases, the cap-shaped bubble with small bubbles tailing becomes irregular. Subsequently, the flow pattern changes from cap-slug flow to churn flow. With the axial height increasing, churn flow develops as wispy annular flow. Meanwhile, the fluid is nearly in the fully developed flashing state, and the axial vapor fraction is increasing slowly. In addition, the transient flow process obtained by the wire-mesh sensor shows that the vapor phase in the pipe center is a continuum, with liquid filament and droplets. The wavy liquid film with uneven thickness flows against the wall and contains scattered small bubbles. The part liquid phase torn by the vapor flow gets up into the vapor core to form a wispy annular flow.



**FIGURE 9: FLOW PATTERN EVOLUTION OF STEADY-STATE FLASHING**



**FIGURE 10: FLOW PATTERN EVOLUTION OF FLASHING-INDUCED INSTABILITIES**

However, the flow pattern evolution is different between the flashing stability flow and flashing instability flow. Under flashing instability flow, slug flow occurs intermittently, and the circulation flow fluctuates violently. With the development of flashing vaporization in the height, the flow pattern changes from bubble flow to slug flow rather than cap-slug flow, as shown in Figure 10. Compared with the cap-slug flow, one of the biggest differences in slug flow is that the length of the vapor

slug gradually becomes longer in the process of flowing upwards and its tail is followed by more and smaller bubbles. During the peak of the flashing-induced oscillation period, the churn flow will occur if the big vapor slug with a long length cannot be maintained under a higher water tank level. The annular flow cannot appear under flashing instability flow because the driving force is not enough to overcome the resistance of the pressure head from the water tank.

#### 4. CONCLUSION

The flashing-induced instabilities were studied in an open NCS. Two types of flow instabilities, the intermittent oscillation between single-phase and two-phase and the flashing-induced oscillation flow were recorded and analyzed. The period and boundary of the flashing-induced oscillation flow was presented for the LUNAR loop. The fluid was in an overheated state of about 0~1.5 °C at the flashing inception. The open NCS was in a stable two-phase flow at  $N_{flash,out} = 4\sim 5$ . The flow pattern evolution of flashing stability flow went through bubble flow, cap-slug flow, churn flow and wispy annular flow. However, the annular flow cannot appear under flashing instability flow. More future works should be done about the pure flashing-induced instabilities in the open NCS. Some sensitive factors causing the FII phenomenon also need to be discussed in detail, such as the structure of the open NCS, the heated power and so on.

#### ACKNOWLEDGEMENTS

The study was sponsored by the National Natural Science Foundation of China (No. 11605033) and was conducted from 2017 to 2018 at Harbin Engineering University. It is very interesting to study the flow flash process in a two-phase flow natural circulation system, so I make these results publicly available. I am expressing my deepest appreciation for the guidance from Professor Cao Xiaxin. Thanks to the help of Mr. Song Ni at the City University of Hong Kong, Mr. Jun Cheng and Ms. Na Li.

#### REFERENCES

- [1] Y. Fang, X. Cao, S. Ni, J. Cheng, and G. Fan, "Study on Flow Pattern with Flow Flashing in Low-Pressure Natural Circulation System," *Atomic Energy Science and Technology* (原子能科学技术), vol. 53, no. 11, pp. 2162–2168, 2019.
- [2] Y. Liao and D. Lucas, "A review on numerical modelling of flashing flow with application to nuclear safety analysis," *Appl Therm Eng*, vol. 182, 2021.
- [3] S. Yin, N. Wang, and H. Wang, "Nucleation and flashing inception in flashing flows: A review and model comparison," *International Journal of Heat and Mass Transfer*, vol. 146, 2020.
- [4] G. A. Pinhasi, A. Ullmann, and A. Dayan, "Modeling of flashing two-phase flow," *Reviews in Chemical Engineering*, vol. 21, pp. 133–164, 2005.
- [5] D. D. B. van Bragt, W. J. M. de Kruijff, A. Manera, T. H. J. J. Van, D. Hagen, and H. van Dam, "Analytical modeling of flashing-induced instabilities in a natural

- circulation cooled boiling water reactor,” *Nuclear Engineering and Design*, vol. 215, pp. 87–98, 2002.
- [6] R. Hu and M. S. Kazimi, “Flashing-induced instability analysis and the start-up of natural circulation boiling water reactors,” *Nucl Technol*, vol. 176, no. 1, pp. 57–71, 2011.
- [7] X. Hou et al., “A study on the steady-state flow behavior of the flashing-driven open natural circulation system,” *Appl Therm Eng*, vol. 182, 2021.
- [8] A. Manera and T. H. J. J. van der Hagen, “Stability of Natural-Circulation-Cooled Boiling Water Reactors during Startup: Experimental Results,” *Nucl Technol*, vol. 143, pp. 77–88, 2003.
- [9] T. Cloppenborg, C. Schuster, and A. Hurtado, “Two-phase flow phenomena along an adiabatic riser - An experimental study at the test-facility GENEVA,” *International Journal of Multiphase Flow*, vol. 72, pp. 112–132, 2015.
- [10] M. Furuya, F. Inada, and T. H. J. J. van der Hagen, “Flashing-induced density wave oscillations in a natural circulation BWR - Mechanism of instability and stability map,” *Nuclear Engineering and Design*, vol. 235, no. 15, pp. 1557–1569, 2005.
- [11] S. Shi, et al., “Experimental investigation of natural circulation instability in a BWR-type small modular reactor,” *Progress in Nuclear Energy*, vol.85, pp. 96–107, 2015.
- [12] X. Hou, Z. Sun, J. Su, and G. Fan, “An investigation on flashing instability induced water hammer in an open natural circulation system,” *Progress in Nuclear Energy*, vol. 93, pp. 418–430, 2016.
- [13] X. Qi, Z. Zhao, P. Ai, P. Chen, Z. Sun, and Z. Meng, “Experiment investigation on flow characteristics of open natural circulation system,” *Nuclear Engineering and Technology*, vol. 54, no. 5, pp. 1851–1859, 2022.
- [14] A. Manera, U. Rohde, H.-M. Prasser, and T. H. J. J. van der Hagen, “Modeling of flashing-induced instabilities in the start-up phase of natural-circulation BWRs using the two-phase flow code FLOCAL,” *Nuclear Engineering and Design*, vol. 235, pp. 1517–1535, 2005.
- [15] Q. Wang, P. Gao, X. Chen, Z. Wang, and Y. Huang, “An investigation on flashing-induced natural circulation instabilities based on RELAP5 code,” *Ann Nucl Energy*, vol. 121, pp. 210–222, 2018.
- [16] Y. Kozmenkov, U. Rohde, and A. Manera, “Validation of the RELAP5 code for the modeling of flashing-induced instabilities under natural-circulation conditions using experimental data from the CIRCUS test facility,” *Nuclear Engineering and Design*, vol. 243, pp. 168–175, 2012.